

# Magnetic Conductive Hydrogel Nanocomposites as Drug Carrier

Issam K. Latif\*, Hilal M. Abdullah, Maida H. Saleem

Department of Chemistry, College of Education for Pure Science /Ibn-Al-Haitham, University of Baghdad, Iraq

**Abstract** Magnetic iron oxide nanoparticles ( $\text{Fe}_3\text{O}_4$  MNPs) were synthesized by co-precipitation method and coated with electrical conductive hydrogel {polyvinyl alcohol (PVA) solution with chitosan (C) and glutaraldehyde (G) as crosslinking agent}/ polyaniline (CPG/PANI). The coated form (CPG/ $\text{Fe}_3\text{O}_4$ /PANI) was loaded with indigo carmine dye which used as drug model, the drug release was tested by using UV-Vis Spectrophotometer at different temperatures (35.5, 37, 38.5) °C and different voltages (3, 5, 8) V in phosphate buffer solution (pH=7.4). The uncoated and coated  $\text{Fe}_3\text{O}_4$  were characterized by FTIR spectra, X-ray diffractions and the average size was found to be about (11-13) nm for uncoated while (12-14) nm for coated form. The surface morphology of coated form (CPG/ $\text{Fe}_3\text{O}_4$ /PANI) was studied by using scanning electron microscope SEM, energy dispersive X-ray spectroscopy (EDS) besides transmission electron microscope (TEM). The (CPG/ $\text{Fe}_3\text{O}_4$ /PANI) show the best releasing at 37 °C.

**Keywords** Magnetic nanoparticles, Drug release, Indigo carmine, Conductive hydrogel, Drug carrying

## 1. Introduction

Nanotechnologies were expanded in many applications and science branches. In medicine was shown new innovations especially in the drug delivery, detection of disease, tissue engineering, biosensors *etc.* Therefore, the design of the nanoparticles must be proper to the applications kind, and in the drug delivery should be suitable for biological activities [1, 2]. The drug delivery depend on the use of microparticles and nanoparticles with important priority such as: (1) decreasing of the drug quantity needed; (2) decreasing the concentration of the drug at nontargeted locations and (3) targeting specific locations in the body [3, 4]. The supplying of anti-tumor compounds to the targeted place which adsorbed with the outer polymer or hydrogel shell of the MNPs, this method is a promising substitution to classical chemotherapy. Reshmi et al. were reported the preparation of colloidal core/shell nanoparticles composite, a biodegradable polymeric shell [5]. The transportation of the drug was with help of the polymeric shell and the releasing could it during its biodegradation [6]. Wei-Chen Huang et al. reported the coating method of electrical responsive hydrogels and the releasing of the drug with applying DC voltages [7]. The coated magnetic nanoparticles were loaded with the drug, the MNPs collected at the infected area by support of outer magnetic field, and then the drugs were be

freed on the infected place [8]. The quantity of drug releasing can be adjusted with external modulation of the electric field. The targeted therapy shows the features of adjusted electric pulses precision, high drug-capacity and targeting, it may be active to enhance the therapeutic effect and to lower toxic effects [9, 10]. The Coating of magnetic nanoparticles with hydrogel or/and polymers utilized for drug delivery was the known way to prevent MNPs oxidation, more over magnetic nanoparticles resort to accumulate due to strong dipole-dipole magnetic attractions and magnetic interactions of the particles [11, 12]. To prevent this difficulty, the aqueous dispersion of the magnetic nanoparticles were coated their surfaces with hydrophilic polymers like chitosan or starch or dextran [13, 14]. Kumar et al. proposed chitosan shell around  $\text{Fe}_2\text{O}_3$  magnetic nanoparticles, and methods for their transport as well concentration to the specific infected area [15].

Electrical conductive polymers [16, 17] and hydrogels [18, 19] were the most favorable materials for the biomedical applications, the first one, because it could be engineered for devices like biosensors, electrically modulated properties [20, 21], substrates for neural prostheses [22, 23] and drug delivery systems [24, 25]. The second ones was due biocompatibility, with high levels of hydration and transport properties [26]. Guiseppi-Elie was described In 1995 the preparation of electro conductive hydrogels (ECHs) as composites or blends [27], the swelling possibility in water was studied experimental and in application, the high diffusivity and biocompatibility show the short molecules of hydrogels with high electrical conductivity an optical and electrical switching, volume changes and electro-chemical

\* Corresponding author:

dr\_issam2003@yahoo.com (Issam K. Latif)

Published online at <http://journal.sapub.org/nn>

Copyright © 2016 Scientific & Academic Publishing. All Rights Reserved

urged to redox properties. Also, Wallace *et al.* were mentioned to the application of controlled release and the preparation of a polyacrylamide/polypyrrole composite [28]. 1) The ECHs almost bend or deswell whilst volume changes under the influence of an electric field. The responsive hydrogels were usually considered diffusion-controlled materials [29, 30]. The influence of the electric field on the ECHs was caused a deswelling and the time of swell again to the equilibrium can only be reached slowly, i.e., hydrogel response to an electric stimulus was slow. The size of the hydrogel deswelling was directly proportional with the electric field magnitude but not linearly [31]. In this work were prepared a conductive nanocomposites hydrogel and used as shell coated iron oxide magnetic nanoparticles core. These ECHs were examined as drug carrying and releasing nanomaterials. Indigo carmine was used as drug model and studied the carrying and releasing properties of the prepared coated MNPs with ECHs.

## 2. Experimental

### 2.1. Materials

Chitosan (CHI) medium average molecular weight, glutaraldehyde solution(25%), (PVA), Sodium dodecyl sulphate ( $\geq 99\%$ ), acetic acid (99%) and aniline were purchased from Sigma-Aldrich, Sulphuric acid and diethyl ether (99.8%) from ROMIL LTD), (from CDH), ammonium persulphate (APS from Hopkin & Williams LTD). All chemicals were of analytical grade and used as received. Double distilled water was used in this work.

### 2.2. Synthesis of Iron Oxide Magnetic Nanoparticles of ( $\text{Fe}_3\text{O}_4$ MNPs)

MNPs ( $\text{Fe}_3\text{O}_4$ ) were synthesized by chemical precipitation, a mixture solution of  $\text{FeSO}_4 \cdot 7\text{H}_2\text{O}$  and  $\text{FeCl}_3$  (molar ratio 1:2) were prepared and sonicated for 1 h under  $\text{N}_2$  shielding and then enough aqueous solution of ammonia was added to this mixture with violently stirring until the PH=10 at  $80^\circ\text{C}$  then added (6ml) of sodium dodecyl sulfate  $\text{NaC}_{12}\text{H}_{25}\text{SO}_4$  (0.4%) to avoid accumulation of the nanoparticles [32]. The black brown precipitate was washed several times with double distilled water to neutralize and finally collected with magnet.

### 2.3. Coating the $\text{Fe}_3\text{O}_4$ MNPs with Conductive Hydrogel

The synthesized hydrogel (CPG) was synthesized according to our previous work [33], but without the step of adding of the crosslinker and performed after the following additions, 1) the dispersed solution of ( $\text{Fe}_3\text{O}_4$  MNPs 2.5 w/w %) was added to the polymers mixture and mixed with ultrasonic device for (1h) and again with the mechanical stirring for (1h) at (2500 rpm.), 2) addition of aniline chloride (30 w/w %) with ammonium persulphate were directly added to the above mixture of (the polymers with MNPs) in ice bath with continues stirring until the color of solution converted

to black green [34]. Then added the crosslinker agent in same concentration for synthesis hydrogel in [33], the mixture was stirred for (1h) at (2500 rpm.), and placed in ultrasonic water bath device for another hour. After completion of reaction, the coated  $\text{Fe}_3\text{O}_4$  with conductive hydrogel composite (CPG/PANI) were collected with magnet and washed several time with distilled water and dried in air then in vacuum oven at ( $40^\circ\text{C}$ ).

### 2.4. Conductivity and Permittivity Measurements

The fabricated ECHs were molded in film form and in pieces which made off  $2 \times 1.5$  cm to fit the silver electrode of the LCR meter Agilent HP Agilent 4284 to measure the Ac conductivity and dielectric properties in frequency range of (100Hz-100 KHz). The complex permittivity was described with the dielectric parameter as a function of frequency by the

$$\varepsilon^*(\omega) = \varepsilon'(\omega) - \varepsilon''(\omega) \quad (1)$$

The  $\varepsilon''$  and  $\varepsilon'$  were represented the imaginary and real permittivity respectively in each cycle of the electrical field. The measured capacitance C was used to calculate the real permittivity  $\varepsilon'$ , using the following expression,

$$\varepsilon' = \frac{Cd}{\varepsilon_0 A} \quad (2)$$

The following symbols were represented the following d the thickness of the measured film, A the area of the studied film and  $\varepsilon_0$  the permittivity of the free space equals to  $8.85 \times 10^{-12} \text{ F.m}^{-1}$ ,

$$(\omega = 2\pi f)$$

$\omega$  and  $f$  were mean the angular frequency and the applied frequency respectively. While for the real and imaginary permittivity  $\varepsilon'(\omega)$ ,  $\varepsilon''(\omega)$  and  $\tan \delta$  was tangent delta,

$$\varepsilon''(\omega) = \varepsilon'(\omega) \cdot \tan \delta(\omega) \quad (3)$$

The (ac) conductivity ( $\sigma_{ac}$ ) calculated with the equation 4 [35].

$$\sigma = \varepsilon_0 \varepsilon' \omega \tan \delta \quad (4)$$

### 2.5. Preparation of the Drug Model Solution

Indigo carmine was used as drug model (fig 1). indigo carmine selected to this work because its own good properties like, intense absorption in the visible range that allows following "in situ" the amount released, high solubility in water, high molar mass and no electrochemical activity with polyaniline in the studied potential range. A standard stock solution of indigo carmine (100 mg/L) was prepared by dissolving (0.01 g) in (100 ml) double distilled water.

Solutions with different concentrations (0.5-5 mg/L) were prepared from the standard stock solution. The absorbance values of different concentrations were measured at the

( $\lambda_{max}$ ) 610 nm for indigo carmine (fig. 2 A). The calibration curve of indigo carmine (absorbance vs. concentration) show the range of concentration obeys Beers-Lambert law (Fig. 2 B).

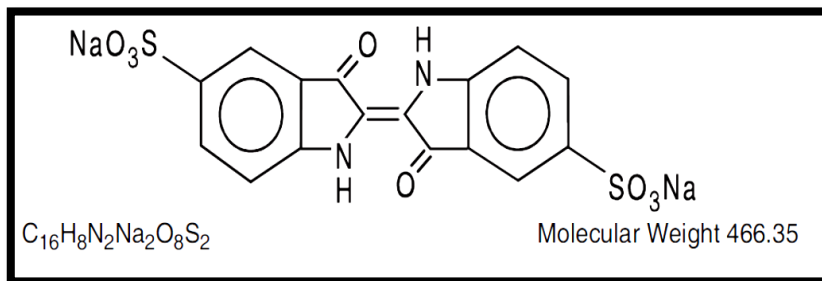


Figure (1). Indigo carmine structure

Table (1). FT-IR frequency values for CPG, PANI,  $Fe_3O_4$  MNPs and its composite

Samples	Wave number( $cm^{-1}$ )	Functional group	Ref.
CPG	3398	O-H hydroxyl group, N-H stretching	[36,37]
	2927&2858	Symmetric and asymmetric CH <sub>2</sub> stretching vibration corresponding to pyranose ring	
	1597	C=N imine group of Schiff base	
	1246	C-N stretching	
	1118	C-O stretching corresponding to secondary alcohol	
	1045	C-O stretching vibration	
PANI	3441	N-H stretching	[38]
	3251	C-H aromatic	
	1554	Quinoid structure	
	1481	Benzenoid structure	
	1300	C-N aromatic	
	1554 to 1743	N-H flexural vibrations	
CPG/PANI	1134	N=Q=N structure	
	3414	O-H hydroxyl group	
	3240	N-H stretching	
	3093	C-H aromatic	
	2858	C-H aliphatic	
	1543	C=N imine group of Schiff base	
	1516	Quinoid structure(Q)	
	1469	Benzenoid structure	
	1288	C-N aromatic	
	1257	C-N aliphatic	
	1184	C-O secondary alcohol	
1130	N=Q=N structure		
1080	C-O stretching vibration to pyranose ring		
$Fe_3O_4$	3412	O-H stretching due to adsorbed water in sample	[39]
	1631	O-H bending vibration	
	628 & 574	Fe-O deformation in octahedral and tetrahedral sites	
CPC/ $Fe_3O_4$ /PANI	3421	O-H , N-H stretching	
	2970	C-H Aromatic overlaps with aliphatic	
	1562	Imine group of Schiff base	
	1512	Quinoid structure	
	1492	Benzenoid structure	
	1296	C-N aromatic	
	1261	C-N aliphatic	
	1176	C-O secondary alcohol	
	1134	N=Q=N structure	
	1083	C-O stretching vibration to pyranose ring	
	636 & 567	Fe-O deformation in octahedral and tetrahedral	

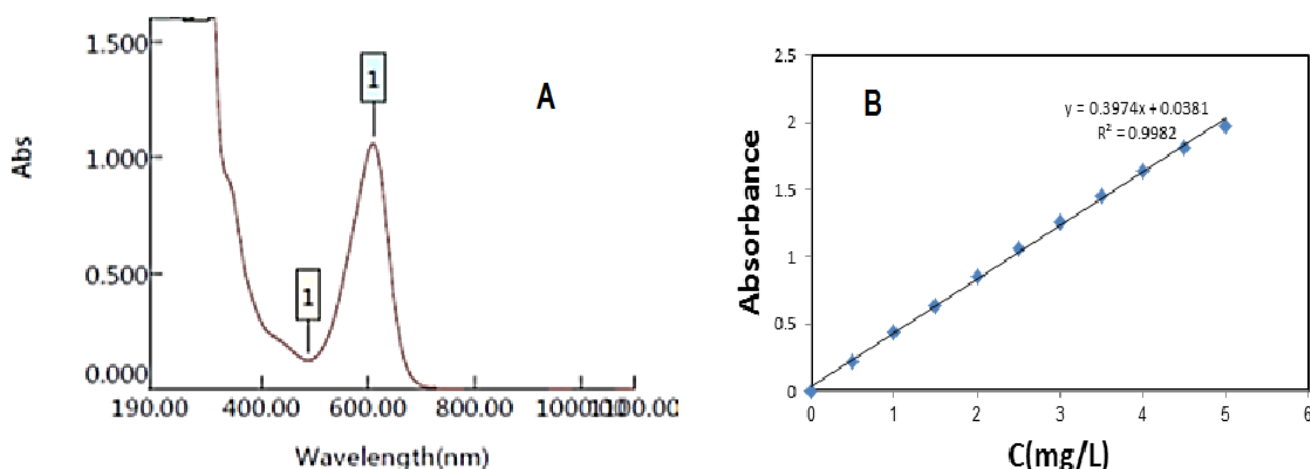


Figure (2). Spectrum of indigo carmine A, Calibration curve of indigo carmine B

## 2.6. Releasing Tests of Indigo Carmine

A desired weight from the conductive hydrogel (CPG/Fe<sub>3</sub>O<sub>4</sub>/PANI) & (CPG/PANI) were dried until reached a stable weight, then it were placed in (5 mg/L) of indigo carmine aqueous solution for 24 h. Then the conductive hydrogel was washed with water and transferred to the electrochemical cell containing 65 mL of a 0.01 M phosphate buffer saline (PBS) pH=7.4. The released amount of indigo carmine in the buffer solution was measured at (610 nm) using UV-Vis spectrophotometer. Electro-liberation curves (concentration of indigo carmine vs. the time) were recorded with the potentials (3, 5, & 8) V & temperatures (35.5, 37, and 38.5) °C.

## 3. Results and Discussion

### 3.1. FTIR Spectroscopy

The FT-IR spectroscopy was a good analytical technique to determine the structure of the hydrogel and the chemical environment present in the polymer associated with different frequencies. The characteristic IR frequencies of CPG, PANI, Fe<sub>3</sub>O<sub>4</sub>, and its composite were shown in the table (1).

### 3.2. XRD Analysis

The crystals structures of Fe<sub>3</sub>O<sub>4</sub> MNPs and composite were examined with XRD, the pure Fe<sub>3</sub>O<sub>4</sub> MNPs in Figures (3-D) was show seven characteristic peaks ( $2\theta = 30.15^\circ, 35.53^\circ, 43.11^\circ, 53.52^\circ, 57.13^\circ, 62.73^\circ$  and  $74.17^\circ$ ) marked by their indices {(220), (311), (400), (422), (511), (440, and 533)} and compared with Joint Committee on Powder Diffraction Standards (JCPDS card, File No. 79-0418) [40]. The average sizes of MNPs were calculated from XRD data using the Debye-Scherrer equation.

$$D = \frac{K\lambda}{\beta \cos \theta} \quad (5)$$

Where,  $K$  (0.91) was Scherrer constant, the X-ray

wavelength (0.15406) was  $\lambda$ ,  $\beta$  was the peak width at half-maximum height (FWHM) and  $\theta$  was the Bragg diffraction angle. The average size of Fe<sub>3</sub>O<sub>4</sub> MNPs was found to be about (11-13) nm. The diffraction pattern of pure PANI has a broad peak around  $2\theta = 25.03$  (fig.3-C) which was a specific peak of PANI [41].

In (Fig.3-B), the diffraction peak of hydrogel (CPG) film has peak around  $2\theta = 19.95$  which is a characteristic peak of CPG hydrogel film. Figure (3-A) showed XRD for (CPG/Fe<sub>3</sub>O<sub>4</sub>/PANI) composite, seven diffraction peaks of Fe<sub>3</sub>O<sub>4</sub> MNPs were appeared also in composite. The peaks intensity of Fe<sub>3</sub>O<sub>4</sub> MNPs composite was lower than pure Fe<sub>3</sub>O<sub>4</sub> MNPs. The broad peak at  $2\theta = 17^\circ$  to  $27^\circ$  in XRD MNPs composite was returned to the hydrogel, mentioned the existence of an amorphous structure [42]. The average size of the coated magnetic nanoparticles form (CPG/Fe<sub>3</sub>O<sub>4</sub>/PANI) was found to be about (13-15) nm.

### 3.3. Surface Morphology and EDS Analysis

#### Scanning electron microscopy

SEM analysis was performed on a FEI electron microscope by using secondary electron beams with energies of 30 keV on samples covered with a thin gold layer. SEM from Zeiss (Jena, Germany) was used to study the surface topography of nanomaterials and hydrogel nanocomposites. The analysis was performed on electron microscope by using secondary electron beams with energies of 15 keV on samples covered with a thin gold layer.

The uncoated Fe<sub>3</sub>O<sub>4</sub> figure (4A) gives a clear picture of coarsely surface in order to the aggregation of the spherical nanoparticles, the coated sample surface appear smother as a result of the ECH (CPG/Fe<sub>3</sub>O<sub>4</sub>/PANI) coating figure (4B).

The EDS analysis of uncoated sample was show the purity of Fe<sub>3</sub>O<sub>4</sub> MNPs, and only the elements Fe and O appeared in the analysis figures 5 (a and b). The SEM & EDS results of coated nanoparticles were shown the type and weight percent of elements present in the selected area of the sample at SEM micrographs figures 5 (c and d),

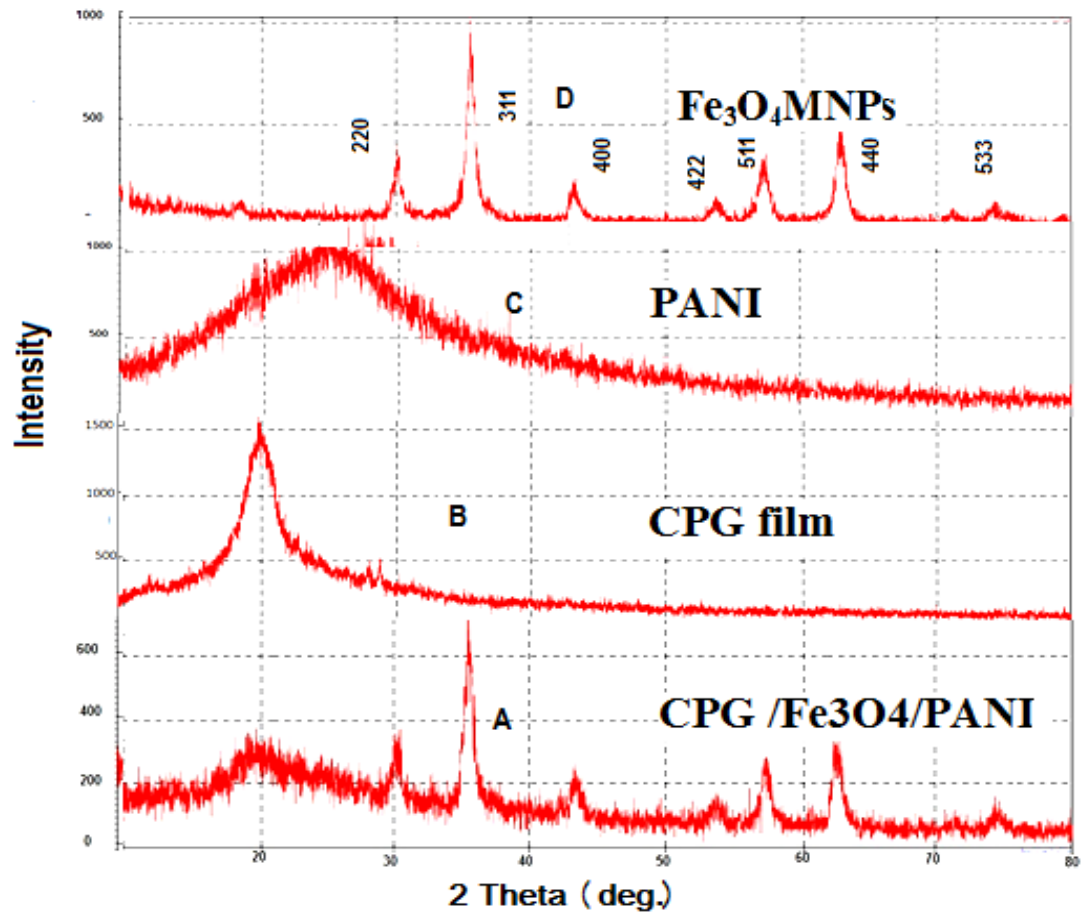


Figure (3). XRD-diffraction of  $\text{Fe}_3\text{O}_4$  MNPs (D), PANI (C), CPG film (B) and CPG/ $\text{Fe}_3\text{O}_4$ /PANI

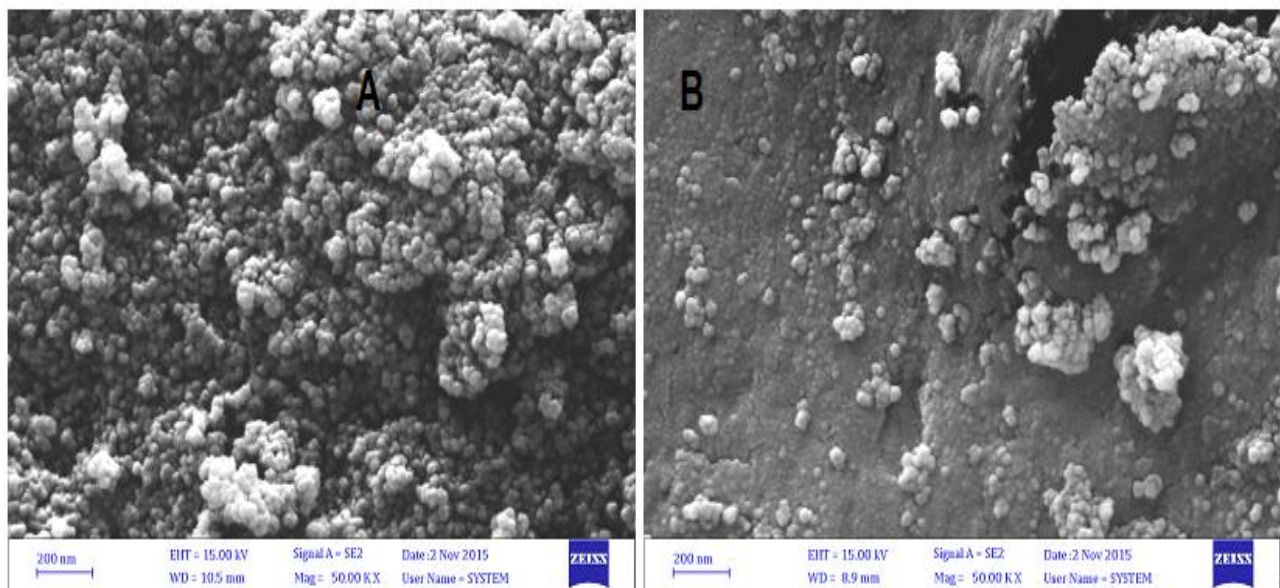
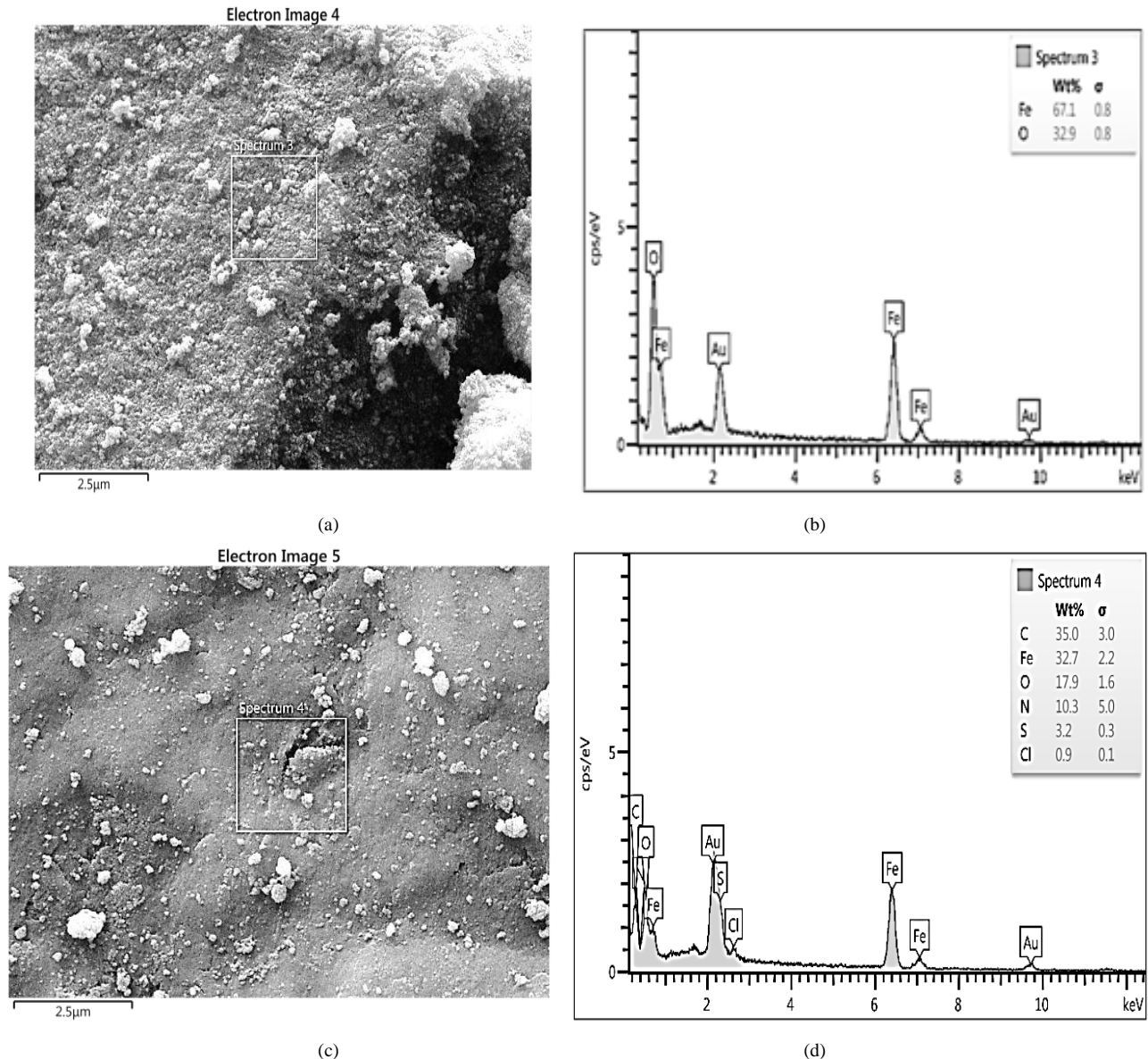


Figure (4). SEM photomicrograph of  $\text{Fe}_3\text{O}_4$  (A), and coated  $\text{Fe}_3\text{O}_4$  (CPG/ $\text{Fe}_3\text{O}_4$ /PANI) (B), with magnification 50 KX



**Figure (5).** Uncoated  $\text{Fe}_3\text{O}_4$  (a) SEM and (b) EDS / coated  $\text{Fe}_3\text{O}_4$  (c) SEM and (d) in form (CPG/ $\text{Fe}_3\text{O}_4$ /PANI)

The EDS analyses were shown and The coated sample analysis consisted new elements (C, N, Cl) due to conductive hydrogel, at the same time was appeared other element (S) with small amount due to the residue of persulphate which used as an oxidizing agent in PANI polymerization. These results indicated a good purity of the prepared materials.

### 3.4. TEM Analysis

The (TEM) images of powdered samples were used a Zeiss-EM10C-80KV high resolution transmission electron microscope. The prepared powder of (CPG/ $\text{Fe}_3\text{O}_4$ /PANI) was dispersed with ultra-sonic device in pure ethanol and for 20 min, then the diluted sample of (CPG/ $\text{Fe}_3\text{O}_4$ /PANI) poured onto a holey carbon-coated copper grid and left to dry before TEM analysis. The size of magnetite nanoparticles

and the morphology was analyzed using TEM. TEM images of uncoated and coated  $\text{Fe}_3\text{O}_4$  nanoparticles showed that the prepared nanoparticles were in a spherical form.

The surface morphology of uncoated  $\text{Fe}_3\text{O}_4$  nanoparticles tends to aggregation due to their high surface energy, magnetization and large specific surface area effect (fig. 6 a). After coating of the magnetic  $\text{Fe}_3\text{O}_4$  nanoparticles with the conductive hydrogel was shown (fig. 6 b) a well coated particles with hydrogel and very clear to recognize the coating and the core of the nanoparticle, the coated nanoparticles were with diameter of nearly 12.66 nm and the shell thickness nearly 3.16 nm, the total diameter of the coated nanoparticles were 19.42 nm this result was agree with XRD results.

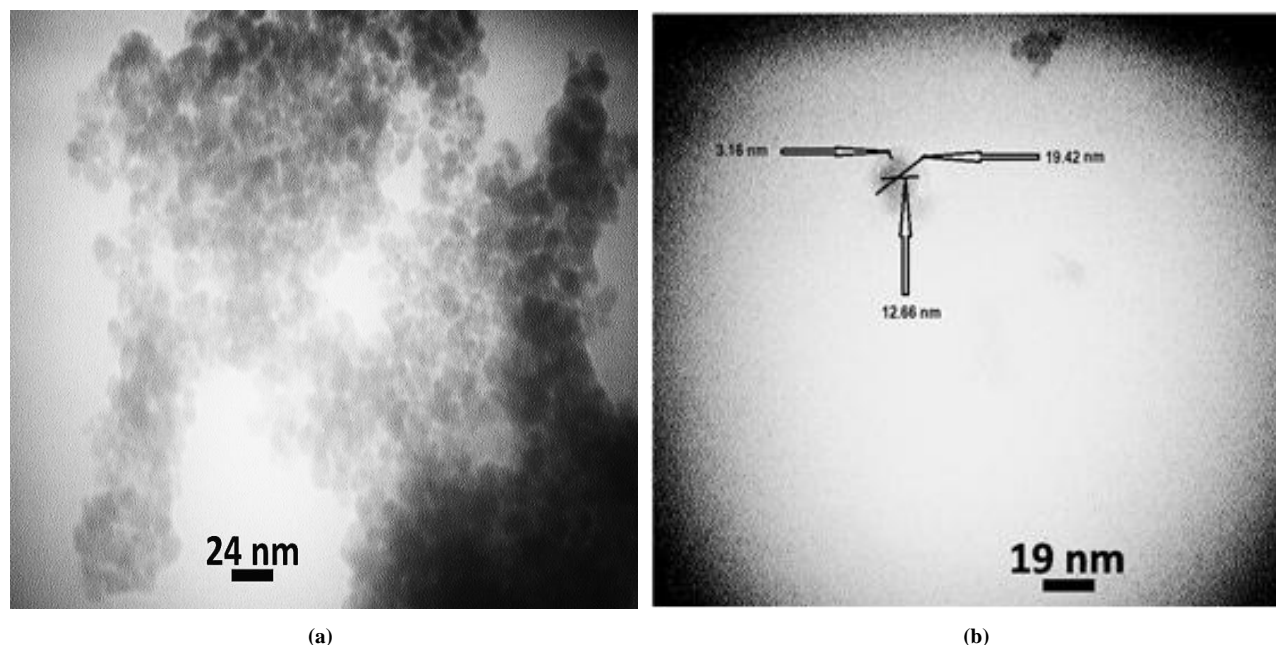


Figure (6). TEM photomicrograph of (a) uncoated  $\text{Fe}_3\text{O}_4$  & (b) coated form (CPG/ $\text{Fe}_3\text{O}_4$ /PANI)

### 3.5. Electric Properties of the Hydrogel Composites

Figure (7) represented the alteration of real permittivity ( $\epsilon'$ ) of hydrogel and hydrogel composite with frequency at room temperature. The permittivity show higher values, in all cases, at low frequencies, which decreased rapidly with increasing of frequency. This is acceptable in the low frequency region the alternation of the field was slow, and that gave sufficient time to induced and permanent dipoles to arrange themselves with the applied field, leading to enhanced polarization. At low frequencies the values of ( $\epsilon'$ ) can be attributed to electrode materials polarization, and/or interfacial polarization. The buildup of space charges at the specimen-electrode materials interface was affected the electrode polarization and characterized with very high values of both real and imaginary part of dielectric permittivity [43-45].

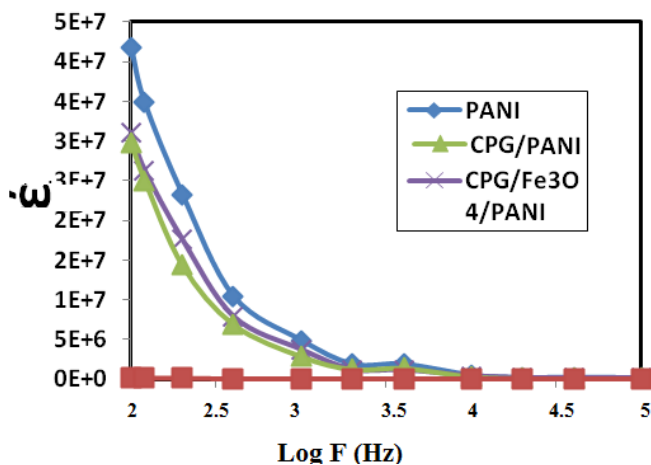


Figure (7). Real permittivity versus log frequency for PANI, CPG/PANI and CPG/ $\text{Fe}_3\text{O}_4$ /PANI composite

Under identical experimental conditions were tested many composition and geometrical characteristics. Thus, if the electrode polarization was the predominant effect in a certain type of nanocomposites, should be also to all other types the predominant tendency. In this case, the higher values of ( $\epsilon'$ ) could be referred to reinforced conductivity and interfacial polarization (IP). The IP results from the aggregation of free charges at the interfaces of the constituents, where they form large dipoles; its intensity was connected to the presence of the existing interfacial area within the composites system, giving thus indirect proof to the achieved distribution of nanomaterials [46].

Dielectric loss ( $\epsilon''$ ) was increased with decreasing of the frequency (Figure 8). On other hand was studied the variation of  $\sigma$  (AC conductivity) with the frequency for the hydrogel and hydrogel composite figure (9). The hydrogel (CPG) show an insulating behavior with the used frequency. While (CPG/PANI) and (CPG/ $\text{Fe}_3\text{O}_4$ /PANI) were show better conductivity because the presence of the polyaniline, this was explained as percolation threshold associated with the formation of conducting network [47]. The electrical conductivity was in this case depends on presence of PANI in the materials and the conductivity increased directly with the frequency, i.e. the conductive polymer was distributed within the hydrogel matrix to form conductive composite, it was created a lot of interfaces areas a large dominate of nomadic electron could provide with large  $\pi$ -orbital of the PANI. When electrons oriented under electric field were the interface polarization can take place. Furthermore, for (CPG/ $\text{Fe}_3\text{O}_4$ /PANI), iron oxide was increased the charge carries and the free volume and also more vacant sites were created for the motion of ions, which in turn enhances the conductivity [48, 49]. Also the figures 7 and 9 show the real permittivity and the Ac conductivity for the (CPG/ $\text{Fe}_3\text{O}_4$ /

PANI) were higher than of the conductive hydrogel alone this may be because the presence of the  $\text{Fe}_3\text{O}_4$  nanoparticles.

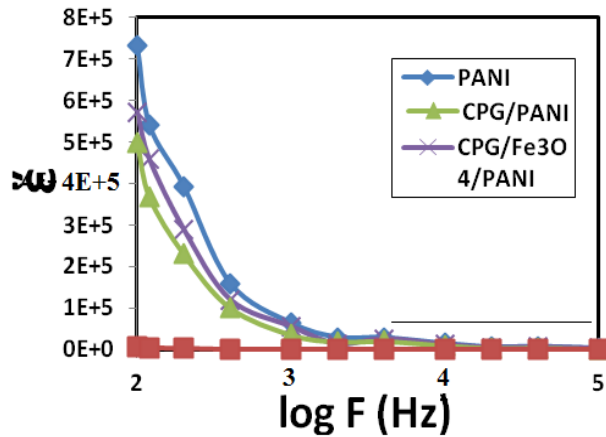


Figure (8). Imaginary permittivity versus log frequency for PANI, CPG/PANI and CPG/ $\text{Fe}_3\text{O}_4$ /PANI composite

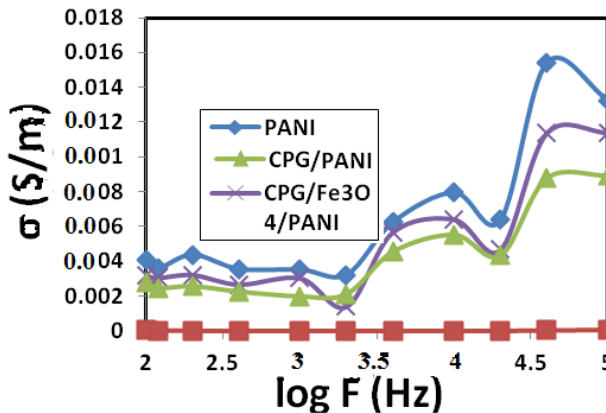
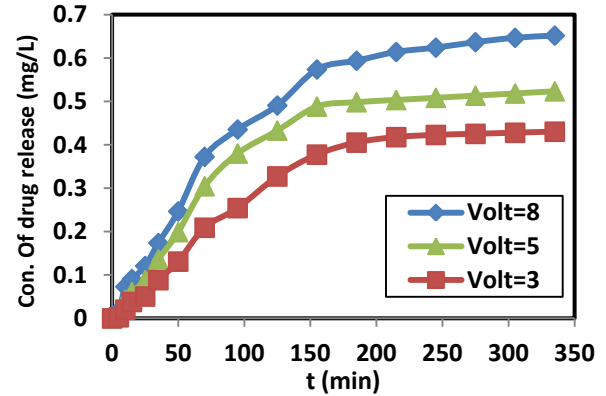


Figure (9). AC conductivity versus log frequency for PANI, CPG/PANI and CPG/ $\text{Fe}_3\text{O}_4$ /PANI composite

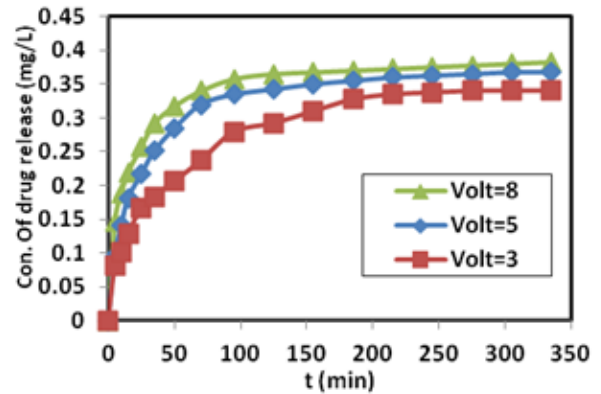
### 3.6. Voltage Optimization for the Drug Releasing

Two gold pieces each  $5 \text{ cm}^2$  were used as a cathode and anode electrode and separated from each other in 1 cm distance. A piece from the conductive hydrogel (0.1g) was fixed its ends with the gold pieces of the electrodes fig.10a, and for the coted magnetic nanoparticles was used an external magnet on the outside wall of the electrochemical cell to collect the coated nanoparticles (CPG/ $\text{Fe}_3\text{O}_4$ /PANI) on the electrodes surface on the inside wall of the electrochemical cell, the total weight of saturated (CPG/ $\text{Fe}_3\text{O}_4$ /PANI) with drug was about 0.1 g also fig.10 (b). The releasing process was studied with different potential ranges (3, 5 and 8 V) using an AC current. At each studied potential difference were totaling about 3 ml PBS in specific time interval from the electrochemical cell and measured with UV-Vis device. The obtained amount of drug release fig 10 (a and b), the figures illustrated the amount of the drug release from the hydrogels which increased with the increasing of voltages values this could be attributed to that the electrons pushed the ionic molecules out and generated small pathways in the hydrogel [50]. The coted magnetic

nanoparticles were show lower releasing of drug than the pristine hydrogel. Even though the coated nanoparticles show a better electrical conductivity than the hydrogel that may be due to the small quantity of the total amount of the hydrogel which coated the magnetic nanoparticles.



(a)



(b)

Figure (10). Drug release profiles showing the influence of various potential differences on the: a: (CPG/PANI) and b: (CPG/ $\text{Fe}_3\text{O}_4$ /PANI)

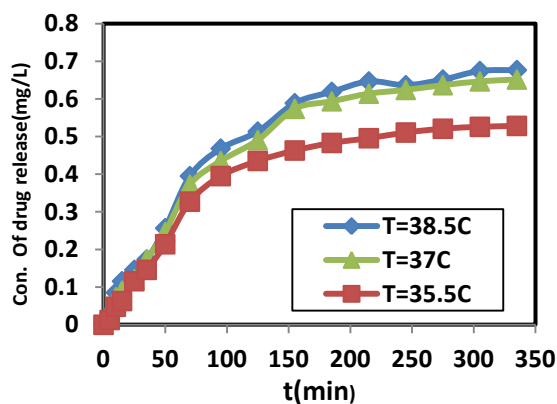
Thus, the higher electric field strength the greater the amount of drugs (indigo) released. On other hand the expansion of hydrogels were directly proportional to the voltage values and affected the pores size in the hydrogel and increased the release of the drugs, the influence electric potential were expanded the conductive hydrogel chains, and a free spaces were generated in the hydrogel matrix, thus the electric field pushing the ionic drug out by electrostatic force. Moreover, the electric field created the micro pathway in the hydrogel while simultaneously expanding the hydrogel mesh size. As a result, the amount and the rate of drug released increase with the applied of external electric field [51 and 56].

### 3.7. Effect of Temperature on the Drug Release

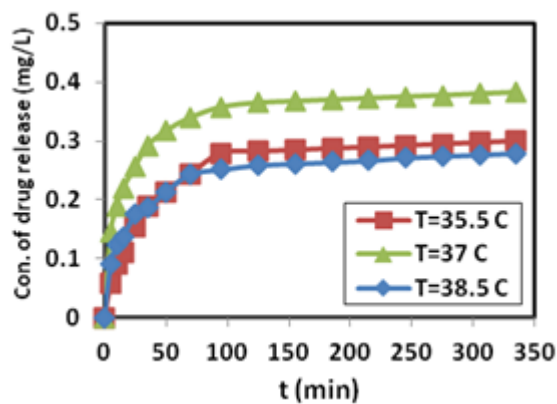
Here the effect of temperature changes on the drug releasing from conductive hydrogel (CPG/PANI) and (CPG/ $\text{Fe}_3\text{O}_4$ /PANI) also was studied. Indigo carmine releasing shown best potential (8V) and at this potential was studied the releasing at different temperatures ranging (35.5,

37, and 38.5 °C). The obtained amounts of drug release were represented in (fig 11).

This figure was demonstrated the highest value of the drug release from (CPG/PANI) and (CPG/Fe<sub>3</sub>O<sub>4</sub>/PANI) hydrogels at 37 °C. This may be due to the hydrogel chains high flexibility at this temperature more than at the other temperatures. Therefore, the drug is released easier and as a consequence the particular nanocarriers can behave as thermo sensitive matrices [52].



(a)



(b)

**Figure (11).** Drug release profiles showing the influence of various temperature differences on the: a: (CPG/PANI) and b: (CPG/Fe<sub>3</sub>O<sub>4</sub>/PANI)

## 4. Conclusions

A spherical Fe<sub>3</sub>O<sub>4</sub> MNPs and coating with conductive hydrogel (CPG/PANI) was successfully synthesized, and they were with very good size. The coated nanoparticles were nearly 20 nm with shell thickness about 3.16 nm this size gives a good opportunity to use these materials in the carrying of drugs. The coated magnetic iron oxide Fe<sub>3</sub>O<sub>4</sub> with electrical conductive hydrogel composite shown better releasing of indigo carmine at the temperature 37°C than the other temperature (humane body temperature). On the other hand, the releasing of drugs was directly proportion with applied electrical current, this makes the hydrogels (CPG/Fe<sub>3</sub>O<sub>4</sub>/PANI) a controllable drugs releasing materials, which gives a good opportunity to use appropriate doses

according to the studied case in clinical treatment..

## REFERENCES

- [1] Gupta AK, Gupta M. Synthesis and surface engineering of iron oxide nanoparticles for biomedical applications. *Biomaterials* 2005; 26: 3995–4021.
- [2] Xie J, Xu CJ, Xu ZC, Hou YL, Young KL, Wang SX, Linking hydrophilic macromolecules to monodisperse magnetite (Fe<sub>3</sub>O<sub>4</sub>) nanoparticles viatrichloro-s-triazine. *Chem Mater* 2006; 18: 5401–3.
- [3] Arruebo M, Fernandez-Pacheco R, Ibarra MR, Santamaria J. Magnetic nanoparticles for drug delivery. *Nano Today* 2007; 2: 22–32.
- [4] Mornet S, Vasseur S, Grasset F, Veverka P, Goglio G, Demourgues Magnetic nanoparticle design for medical applications. In: Meeting of the European-Materials-Research-Society. Strasbourg, France: Pergamon-Elsevier Science Ltd.; 2005. p. 237–47.
- [5] Reshmi G, Kumar PM, Malathi M. Preparation, characterization and dielectric studies on carbonyl iron/cellulose acetate hydrogen phthalate core/shell nanoparticles for drug delivery applications. *Int J Pharm* 2009; 365: 131–5.
- [6] Arias JL, Lopez-Viota M, Ruiz MA, Lopez-Viota J, Delgado AV. Development of carbonyl iron/ethylcellulose core/shell nanoparticles for biomedical applications. *Int J Pharm* 2007; 339: 237–45.
- [7] Wei-Chen Huang, Tai-Jung Lee, Chi-Sheng Hsiao, San-Yuan Chen and Dean-Mo Liu. Characterization and drug release behavior of chip-like amphiphilic chitosan–silica hybrid hydrogel for electrically modulated release of ethosuximide. *J.Mater. Chem.*, 2011,21, 16077-16085
- [8] Fernandez-Pacheco R, Marquina C, Valdivia JG, Gutierrez M, Romero MS, Cornudella R. Magnetic nanoparticles for local drug delivery using magnetic implants. In: 6th international conference on the scientific and clinical applications of magnetic carriers. Elsevier Science B.V.; 2006. p. 318–22.
- [9] Cregg PJ, Murphy K, Mardinoglu A. Calculation of nanoparticle capture efficiency in magnetic drug targeting. *J Magn Magn Mater* 2008; 320: 3272–5.
- [10] Wang D, Li J, Li H, Tang F. Preparation and drug releasing property of magnetic chitosan-5-fluorouracil nano-particles. *Trans Nonferrous Metals Soc China* 2009; 19:1232–6.
- [11] Faraji A, Wipf P. Nanoparticles in cellular drug delivery. *Bioorg Med Chem* 2009; 17:2950–62.
- [12] Singh R, Lillard JW. Nanoparticle-based targeted drug delivery. *Exp Mol Pathol* 2009; 86:215–23.
- [13] Bhattarai SR, Badahur KCR, Aryal S, Khil MS, Kim HY. N-acylated chitosan stabilized iron oxide nanoparticles as a novel nano-matrix and ceramic modification. *Carbohydr Polym* 2007; 69: 467–77.
- [14] Chertok B, Moffat BA, David AE, Yu FQ, Bergemann C, Ross BD, et al. Iron oxide nanoparticles as a drug delivery

- vehicle for MRI-monitored magnetic targeting of brain tumors. *Biomaterials* 2008; 29:487-96.
- [15] Kumar A, Jena P, Behera S, Lockey R, Mohapatra S, Mohapatra S. Multifunctional magnetic nanoparticles for targeted delivery. *Nanomedicine* 2009:1-6.
- [16] M. Asplund, T. Nyberg and O. Inganäs, "Electroactive Polymers for Neutral Interfaces," *Polymer Chemistry*, Vol. 1, No. 9, 2010, pp. 1374-1391. doi:10.1039/c0py00077a.
- [17] T. Skotheim and J. R. Reynolds, "Handbook of Conducting Polymers: Conjugated Polymers Processing and Applications 3rd Edition," Taylor and Francis, New York, 2007.
- [18] S. H. Gehrke and P. I. Lee, "Hydrogels for Drug Delivery Systems," In: P. Tyle, Ed., *Specialized Drug Delivery Systems*, Marcel Dekker, New York, 1990, pp. 333-392.
- [19] P. Gupta, K. Vermani and S. Garg, "Hydrogels: From Controlled Release to pH Responsive Drug Delivery," *Drug Discovery Today*, Vol. 7, No. 10, 2002, pp. 569-579.
- [20] N. Wisniewski, F. Moussy and W. M. Reichert, "Characterization of Implantable Biosensors Membrane Bio-filing," *Fresenius' Journal of Analytical Chemistry*, Vol. 366, 2000, pp. 611-621.
- [21] O. M. Schuvailo, O. O. Soldatkin, A. Lefebvre, R. Cespuglio and A. P. Soldatkin, "Highly Selective Micro-biosensors for in Vivo Measurement of Glucose, Lactate and Glutamate," *Analytical Chimica Acta*, Vol. 573-574, 2006, pp. 110-116. doi:10.1016/j.aca.2006.03.034
- [22] P. M. George, A. W. Lyckman, D. A. LaVan, A. Hegde, Y. Leung, R. Avasare, C. Testa, P. M. Alexander, R. Langer and M. Sur, "Fabrication and Biocompatibility of Polypyrrole Implants Suitable for Neural Prosthetics," *Biomaterials*, Vol. 26, No. 17, 2005, pp. 3511-319.
- [23] X. Cui, J. Wiler, M. Dzaman, R. A. Altschuler and D. C. Martin, "In Vivo Studies of Polypyrrole/Peptide Coated Neural Probes," *Biomaterials*, Vol. 24, No. 5, 2003, pp. 777-787. doi:10.1016/S0142-9612(02)00415-5.
- [24] B. Zinger and L. L. Miller, "Timed Release of Chemicals from Polypyrrole Films," *Journal of the American Chemical Society*, Vol. 106, No. 22, 1984, pp. 6861-6863. doi:10.1021/ja00334a076.
- [25] N. K. Lau and L. L. Miller, "Electrochemical Behavior of a Dopamine Polymer. Dopamine Release as a Primitive Analog of a Synapse," *Journal of the American Chemical Society*, Vol. 105, No. 16, 1983, pp. 5271-5277. doi:10.1021/ja00354a016.
- [26] S. Murdan, "Electro-Responsive Drug Delivery from Hydrogels," *Journal of Controlled Release*, Vol. 91, 1994, pp. 3201-3204.
- [27] A. Guiseppi-Elie and N. F. Sheppard Jr., "Conferrig Bio-specificity to Electroconductive Polymer-Based Biosensors Devices," *ACS Northeast Regional Meeting (NERM)*, Rochester, October 1995, pp. 22-25.
- [28] C. J. Small, C. O. Too and G. G. Wallace, "Responsive Conducting Polymer-Hydrogel Composites," *Polymer Gels and Network*, Vol. 5, No. 3, 1997, pp. 251-265. doi:10.1016/S0966-7822(96)00044-5.
- [29] B. Zinger and L. L. Miller, "Timed Release of Chemicals from Polypyrrole Films," *Journal of the American Chemical Society*, Vol. 106, No. 22, 1984, pp. 6861-6863. doi:10.1021/ja00334a076.
- [30] A.N. K. Lau and L. L. Miller, "Electrochemical Behavior of a Dopamine Polymer. Dopamine Release as a Primitive Analog of a Synapse," *Journal of the American Chemical Society*, Vol. 105, No. 16, 1983, pp. 5271-5277. doi:10.1021/ja00354a016.
- [31] X. Cui, V. A. Lee, Y. Raphael, J. A. Wiler, J. F. Hetke, D. J. Anderson and D. C. Martin, "Surface Modification of Neutral Recording Electrodes with Conducting Polymer/Biomolecule Blends," *Journal of Biomedical Materials Research*, Vol. 56, No. 2, 2001, pp. 261-272.
- [32] J. Liu, J. Shi, L. Jiang, F. Zhang, L. Wang, & S. Yamamoto, Segmented magnetic nanofibers for single cell manipulation, *Appl. Surf. Sci.*, Vol. 258, 7530-7535, (2012).
- [33] Issam A. Latif, Hilal M. Abdullah, Maida Hameed Saleem, Electrical and Swelling Study of Different Prepared Hydrogel. *American Journal of Polymer Science* 2016, 6(2): 50-57.
- [34] J. Stejskal & R. G. Gilbert, Polyaniline. Preparation of a conducting Polymer (IUPAC Technical Report), *Pure Appl. Chem.*, Vol. 74, No. 5, 857-867, (2002).
- [35] Seyfullah Madakbas, Kadir Esmer, Ersin Kayahan, & Mehmet Yumak "Synthesis and Dielectric Properties of Poly(aniline)/Na-bentonite Nanocomposite", *Science and Engineering of Composite Materials* 17, 145-153(2010).
- [36] U. Edlund, and A. C. Albertsson, "Degradable Polymer Microspheres for Controlled Drug Delivery," *Advances in Polymer Science*, Vol. 157, 67-112(2002).
- [37] D. Sahoo, S. Sahoo, J. Das, T. K. Dangar and P. L. Nayak, "Antibacterial Activity of Chitosan Crosslinked with Aldehydes and Blended with Cloisite 30B," *NanoTrends*, Vol. 10, 1-9(2011).
- [38] Sajjad Sedaghat, Synthesis and characterization of new bio compatible copolymer: chitosan -graft-polyaniline, *International Nano Letters*, 4: 2, 1-6 (2014).
- [39] Karina Donadel, Marcos D.V. Felisberto, Valfredo T. Favere, Mauricio Rigoni, Nelson Jhoé Batistela, Mauro C.M. Laranjeira, Synthesis and characterization of the iron oxide magnetic particles coated with chitosan biopolymer, *Materials Science and Engineering C* 28, 509-514(2008).
- [40] Liang Guo, Guang Liu, Ruo-Yu Hong, and Hong-Zhong Li, Preparation and Characterization of Chitosan Poly(acrylic acid) Magnetic Microspheres, *Mar. Drugs*, 8, 2212-2222 (2010).
- [41] A. R. Subrahmanyam, V. Geetha, Atul kumar, A. Alakanandana, J. Siva Kumar, Mechanical and Electrical Conductivity Studies of PANI-PVA and PANI-PEO Blends, *International Journal of Material Science*, Vol.2, Iss.1, PP.27-30(2012).
- [42] Liu L, Xiao L, Zhu HY, & Shi XW, Preparation of magnetic and fluorescent bifunctional chitosan nanoparticles for optical determination of copper ion. *Microchim Acta*, 178(3): 413-419 (2012).
- [43] Tsangaris GM, Psarras GC, & Kouloumbi N "Polyurethane

- latex/water dispersible boehmite alumina nanocomposites: Thermal, mechanical and dielectrical properties", *Journal of Materials Science*, vol. 33, no.8, 2027-2037, (1998).
- [44] K.G. Gatos, J.G. Martinez Alcazar, G.C. Psarras, R. Thomann, & J. Karger-Kocsis, Polyurethane latex/water dispersible boehmite alumina nanocomposites: thermal mechanical and dielectrical properties, *Composites Science and Technology* 67 (2) 157–167(2007).
- [45] Psarras GC, Gatos KG, Karahaliou PK, Georga SN, Krontiras CA, & Karger-Kocsis J "Relaxation phenomena in rubber/layered silicate nanocomposites", Springer, *Express Polymer Letters*, vol. 1, 837-845(2007).
- [46] Kalini A, Gatos KG, Karahaliou PK, Georga S N, Krontiras CA, & Psarras GC "Probing the dielectric response of polyurethane/alumina nanocomposites", *Journal of Polymer Science Part B: Polymer Physics*, vol. 48, 2346-2354 (2010).
- [47] Li YC, Li RKY, & Tjong SC "Frequency and temperature dependences of dielectric dispersion and electrical properties of polyvinylidene fluoride/expanded graphite composites "javascript; Springer, *Journal of Nanomaterials*, no vol., and pp. given, (2010).
- [48] Dang Z, Wang L, Yin Y, Zhang Q, Lei Q "Giant dielectric permittivities in functionalized carbonnanotube/ electroactive - polymer nanocomposites", Wiley, *Advanced Materials*, vol. 19, pp.852-857, (2007).
- [49] S. Devikala, P. Kamaraj and M. Arthanareeswari, Conductivity and Dielectric Studies of PMMA Composites, *Chem Sci Trans.*, 2(S1), S129-S134 (2013).
- [50] Bajpai, A.K., Shukla, S.K., Bhanu, S., & Kankane, S., "Responsive polymers in controlled drug delivery". *Prog. Polym. Sci.*, 33, 1088–1118(2008).
- [51] Li Y., Neoh K.G., Kang E.T., Controlled release of heparin from polypyrrole-poly(vinyl alcohol) assembly by electrical stimulation. *J. Biomed. Mater. Res.*, 73A, 171–181(2005).
- [52] M. Filippousi, T. Altantzis, G. Stefanou, M. Betsiou, D. N. Bikiaris, M. Angelakeris, E. Pavlidou, D. Zamboulis and G. Van Tendeloo, "Polyhedral iron oxide core-shell nanoparticles in a biodegradable polymeric matrix: preparation, characterization and application in magnetic particle hyperthermia and drug delivery", *RSC Adv.*, 3, 24367–24377.